THE DEFORMATION OF SOLITARY WAVES ON STEEP SLOPES

Chung-Ren Chou* and Kwan Ouyang
Department of Harbor and River Engineering
Taiwan Ocean University
Keelung, Taiwan 202, R.O.C.

ABSTRACT

The phenomenon of solitary waves propagating through steep slopes is numerically analyzed by means of the boundary element method. With the fully nonlinear boundary condition on the free water surface, the Lagrangian method is used in the numerical scheme to describe the motion of the fluid particles. The forward-difference approximation is used to deal with the time derivative. The processes of runup and rundown of solitary waves on steep slopes are studied. Present results are compared to other published results. For waves with a ratio of incident wave height to water depth, 0.4, the distributions of fluid velocities are presented.

I. INTRODUCTION

For the design of coastal structures, the propagation and runup of solitary waves over shelf and slope is one of the most important investigations. Based on the Boussinesq equation, the numerical simulations for runup of solitary waves are studied by Pedersen and Gjevik (1983), Kim *et al.* (1983). Synolakis (1987) and Kobayashi *et al.* (1989) studied the runup of solitary waves using first order nonlinear shallow water wave equations.

Based on potential flow, the boundary element method with fully nonlinear boundary conditions has been developed by many researchers. Nakayama (1983) analyzed the propagation of tsunami and runup of a solitary wave against a vertical wall. Grilli *et al.* (1994a, 1997) investigated the breaking of solitary waves on slopes. The characteristics of solitary waves breaking on immerged or submerged breakwaters have also been studied by Grilli *et al.* (1994b). One of the authors (Chou & Shih, 1996) analyzed the generation and deformation of solitary waves on

slopes; the scattering problems induced by the waves over the shallow water region were also discussed.

As shown in Fig. 1, Street and Camfield (1966) studied the runup of solitary waves and presented the criterion of breaking type and limitation of wave height by laboratory investigation. They found that, for solitary waves on the slope greater than $10°$, waves would not break during runup. Grilli *et al.* (1994b) studied the rundown of solitary waves on slope $s=1:2$ and reported that waves may break during rundown. In these papers, however, the distribution of fluid velocity was not fully discussed.

In this paper, the runup and rundown of solitary waves on steep slopes are numerically analyzed. On various steep slopes (slope=1:1, 1:2 and 1:5), solitary waves with relative incident wave height $H'_o = H_o/h_o=0.2$, 0.3 and 0.4 are studied, where H_o and h_o denote incident wave height and the water depth of constant water region, respectively. For the case of $H'_o=0.4$, the distributions of fluid velocities are also presented.
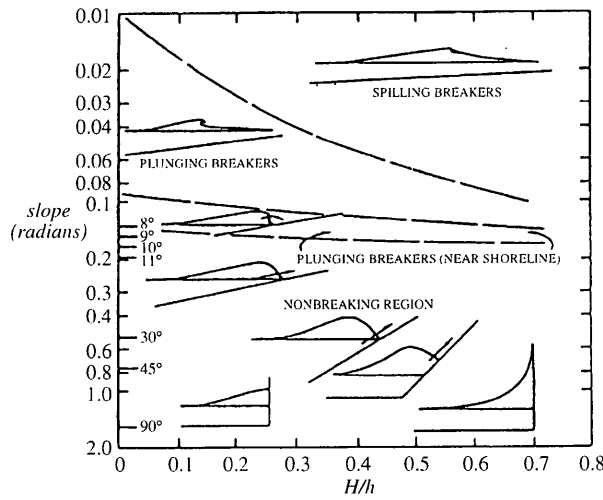
---

*Correspondence addressee

Fig. 1. The criterion of breaking type of solitary waves published by Street & Camfield (1966).

II. THEORETICAL ANALYSIS

A numerical wave tank diagram is shown in Fig. 2. The origin of the coordinate is located at the intersection of still water surface and slope. The x-axis and z-axis are pointed positively right and upwards, respectively. The fluid domain is bounded by the pseudo wave generator Γ_1, free water surface Γ_2, impermeable slope Γ_3, and seabed Γ_4.

1. Governing Equation

Assuming that the fluid is inviscid and incompressible, and the flow is irrotational, the velocity potential $\Phi(x, z; t)$ must satisfy the following Laplace equation:

$$\frac{\partial^2\Phi}{\partial x^2} + \frac{\partial^2\Phi}{\partial z^2} = 0 \qquad (1)$$

2. Boundary Conditions

(i) Pseudo Wave Generator Γ_1:

A piston type of wave generator is modeled. The fluid velocity normal to the paddle should be the same as the horizontal moving velocity of the wave generator $U(t)$:

$$\overline{\Phi} = \frac{\partial\Phi}{\partial n} = -U(t), \text{ on } \Gamma_1 \qquad (2)$$

where n denotes the unit outward normal.

(ii) Free Water Surface Γ_2:

Assuming that the atmospheric pressure on the free water surface is constant and equal to zero, the
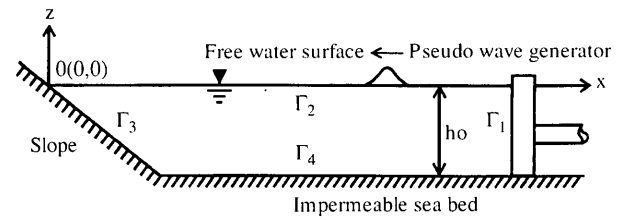

Fig. 2. Diagram of a numerical wave tank.

Bernoulli equation can be expressed as

$$\frac{D\Phi}{Dt} + g\zeta - \frac{1}{2}[(\frac{\partial\Phi}{\partial x})^2 + (\frac{\partial\Phi}{\partial z})^2] = 0, \text{ on } \Gamma_2 \qquad (3)$$

where D denotes the Lagrangian differentiation, g is the gravitational acceleration and ζ is the elevation of free water surface.

(iii) Impermeable Slope Γ_3 and Seabed Γ_4:

Since these boundaries are assumed to be impermeable, the velocity normal to boundaries is equal to zero.

$$\frac{\partial\Phi}{\partial z} = 0, \text{ on } \Gamma_3, \Gamma_4 \qquad (4)$$

3. Initial Boundary Conditions

For simulating the generation of a solitary wave, $U(t)$ in Eq. (2) can be expressed as

$$U(t) = x_0 \cdot \omega \cdot \sec h_o^2[\omega(t - t_c)] \qquad (5)$$

$$x_0 = h_0\sqrt{\frac{4H_o}{3(h_0 + H_0)}} \qquad (6)$$

$$\omega = \sqrt{\frac{g}{h_0}} \sqrt{\frac{3H_o}{4h_0}(1 + \frac{H_o}{h_0})} \qquad (7)$$

$$t_c = \frac{\pi}{\omega} \qquad (8)$$

where x_0 is a semistroke of the paddle, t_c is a characteristic time, ω is a characteristic angular frequency. The initial normal derivative of velocity potential on the pseudo wave generator is

$$\overline{\Phi}_1^0 = \frac{\partial\Phi_1^0}{\partial n} = U(0) \qquad (9)$$

where the subscript denotes the boundary and the superscript denotes the time step. Assuming the free water surface is undisturbed at $t=0$, the initial velocity potential of the free water surface is

$$\Phi_2^0 = 0 \qquad (10)$$

Since the boundaries of the slope and seabed are impermeable, the normal fluid velocities are zero at any time:

$$\overline{\Phi}_k^0 = \frac{\partial \Phi_k^0}{\partial n} = 0 \quad k=3,4 \tag{11}$$

3. NUMERICAL METHOD

1. Integral Equation

If the velocity potential satisfies the Laplace equation and its second derivative exists, according to Green's Second Identity, the velocity potential in the fluid domain $\Phi(x, z; t)$ can be obtained by the velocity potential on the boundary $\Phi(\xi, \eta; t)$, and its normal derivative, $\partial \Phi(\xi, \eta; t)/\partial n$, i.e.

$$\Phi(x, z; t) = \frac{1}{2\pi} \int_\Gamma [\frac{\partial \Phi(\xi, \eta; t)}{\partial n} \ln \frac{1}{r} - \Phi(\xi, \eta; t) \frac{\partial}{\partial n} \ln \frac{1}{r}] ds \tag{12}$$

where $r=[(\xi-x)^2+(\eta-z)^2]^{1/2}$. When (x, z) approaches to the smooth boundary (ξ', η'), due to the singularity, the velocity potential $\Phi(\xi', \eta'; t)$ can be expressed as

$$\Phi(\xi', \eta'; t) = \frac{1}{\pi} \int_\Gamma [\frac{\partial \Phi(\xi, \eta; t)}{\partial n} \ln \frac{1}{R} - \Phi(\xi, \eta; t) \frac{\partial}{\partial n} \ln \frac{1}{R}] ds \tag{13}$$

where $R=[(\xi-\xi')^2+(\eta-\eta')^2]^{1/2}$.

2. Discretization for Integral Equation

In order to solve the integral equation numerically, the boundaries Γ_1 through Γ_4 are divided into N_1 to N_4 discrete segments respectively with linear elements, and the integral equation can be written in a matrix form as:

$$[\Phi]=[O][\overline{\Phi}] \tag{14}$$

where $[\Phi]$ is the velocity potential, $[\overline{\Phi}]$ is the normal derivative of velocity potential on the boundary, $[O]$ is a matrix of the relative shape function. The details can be checked in Chou (1983).

3. The Forward-Difference of the Time Derivative

Based on the Lagrangian description and the definition of velocity potential, we can obtain the following equations:

$$u = \frac{Dx}{Dt} = \frac{\partial \Phi}{\partial x} \tag{15}$$

$$w = \frac{Dz}{Dt} = \frac{\partial \Phi}{\partial z} \tag{16}$$

where u and w are horizontal and vertical components of fluid velocity, respectively. To deal with the time derivative in Eq. (15) and Eq. (16), the forward-difference approximation is adopted. At the $k+1$-th time step, the free water surface (x^{k+1}, z^{k+1}) can be obtained by the following equations.

$$x^{k+1} = x^k + (\frac{\partial \Phi_2^k}{\partial x})\Delta t \tag{17}$$

$$z^{k+1} = z^k + (\frac{\partial \Phi_2^k}{\partial z})\Delta t \tag{18}$$

The velocity potential on free water surface at $k+1$-th time step can be obtained from Eq. (3):

$$\Phi_2^{k+1} = \Phi_2^k + \frac{1}{2}[(\frac{\partial \Phi_2}{\partial s})^2 + (\frac{\partial \Phi_2}{\partial n})^2]^k \Delta t - gz^{k+1}\Delta t \tag{19}$$

4. The Distribution of Fluid Velocity

The fluid velocity in the fluid domain can be derived from the velocity potential and its normal derivative on boundary as follows.

$$u = \frac{\partial \Phi(x, z; t)}{\partial x}$$

$$= \frac{1}{2\pi} \int_\Gamma \{\frac{\partial \Phi(\xi, \eta; t)}{\partial n}(\frac{\xi-x}{r^2})$$

$$- \Phi(\xi, \eta; t)[\frac{\partial x}{\partial n}(\frac{1}{r^2} - \frac{2(\xi-x)^2}{r^4}) - \frac{\partial z}{\partial n}(\frac{2(\xi-x)(\eta-z)}{r^4})]\} d\Gamma \tag{20}$$

$$w = \frac{\partial \Phi(x, z; t)}{\partial z}$$

$$= \frac{1}{2\pi} \int_\Gamma \{\frac{\partial \Phi(\xi, \eta; t)}{\partial n}(\frac{\eta-z}{r^2})$$

$$- \Phi(\xi, \eta; t)[\frac{\partial z}{\partial n}(\frac{1}{r^2} - \frac{2(\eta-z)^2}{r^4}) - \frac{\partial z}{\partial n}(\frac{2(\xi-x)(\eta-z)}{r^4})]\} d\Gamma \tag{21}$$

5. The Distribution of Elements

Figure 3 represents the sketch of the distribution of elements. Linear element is adopted. N_1, N_2, N_3 and N_4 denote the numbers of elements on the pseudo wave generator, the free water surface, the slope and the seabed, respectively. At the beginning, for the pseudo wave generator, slope and seabed, the
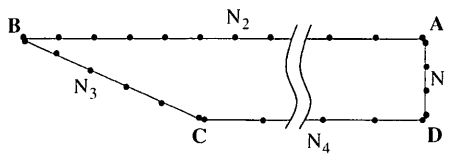
Fig. 3. Sketch for the distribution of elements.

Table 1. Distributions of Elements for Variant Slopes

	$s=1:1$	$s=1:2$	$s=1:5$
N_1	20	20	20
N_2	59	61	67
N_3	10	20	20
N_4	120	120	120

elements on each boundary are equally discretized. On the free water surface, the length of element $\Delta s=1.0h_o$ is used for the first three elements near the pseudo wave generator to reduce the time interval of numerical computation, $\Delta s=0.5h_o$ for others. For various slopes, the distributions of elements are listed in Table 1. The water depth of the constant water region h_o is 1m and the distance of the constant water region is taken to be 30 h_o. Double nodes technique (Chou, 1988) is applied to the corner problem on boundaries which have two different boundary conditions on the corner, e.g. location A, B, C and D in Fig. 3.

IV. NUMERICAL RESULTS AND DISCUSSION

1. Runup and Rundown on slopes s=1:1 and 1:2

The solitary waves approaching the slopes of $s=1:1$ and 1:2 are studied first. Time interval $\Delta t=t_c/200$ is adopted first, and $\Delta t=t_c/200$ is used after $t=4t_c$, $5t_c$ and $6t_c$ for $H'_o=0.2$, 0.3 and 0.4, respectively.

The solitary waves propagate through the constant water region and rush up the slope without breaking. The dimensionless maximum runup is listed in Table 2. The maximum runup $R'=R/h_o$ denotes the vertical distance between the still water level and the intersection of the free water surface and the slope. To investigate the accuracy of the present numerical scheme, the numerical results are compared with a runup formula derived by Synolakis (1987) as

$$R' = 2.831(\cot\beta)^{\frac{1}{2}}(H_o/h_o)^{\frac{5}{4}} \qquad (23)$$

where β is the slope angle. For the case of $s=1:2$, numerical results obtained by Grilli *et al.* (1994) are also listed. Comparing present results to the runup formula, for the case of $s=1:1$, reasonable agreement is observed. For the case of $s=1:2$, the maximum runup is smaller than others. When solitary waves reach the maximum runup, the profiles of the free water surface are shown in Fig. 4a and Fig. 4b for the slopes $s=1:1$ and 1:2, respectively. For slope $s=1:2$, the results obtained by Grilli *et al.* (1994) are also presented. Solid and dashed lines denote present results and Grilli's, respectively.

Figure 5a shows the rundown of solitary waves on slope $s=1:1$. It is found that, except for the case

of $H'_o=0.4$, waves break under still water level. For slope $s=1:2$, Fig. 5b shows present results (solid line) and Grilli's (1994) results (dashed line). The difference is due to numerical techniques. In our scheme, a linear element is applied; in Grilli's scheme, cubic spline element and regridding technique are used. More details for $H'_o=0.4$ on slopes $s=1:1$ and 1:2 will be discussed in section 4.4.

3. Solitary Waves on Slope s=1:5

Figure 1, Street and Camfield (1966) indicates that solitary waves on slope $s=1:5$ may break during runup. In this paper, the waves with $H'_o=0.2\sim0.4$ are studied. Time interval $\Delta t=t_c/200$ is adopted first for all cases. For the cases of $H'_o=0.2$ and 0.3, $\Delta t=t_c/1000$ is used after $t=5t_c$, for the case of $H'_o=0.4$ $\Delta t=t_c/2000$ is used after $t=6t_c$. Some breaking criteria for solitary waves are usually used: (1) the velocities of water particles on the wave crest is equal to the celerity of the wave; (2) the angle of water surface profile on the crest is less than 120^0; (3) the vertical tangent occurs on the front of the wave profile; (4) the ratio of wave height to water depth achieves a specific value, namely the related breaking wave height $H'_b=H_b/h_b$, where the subscript b denotes the values at breaking. For the related breaking wave height, many different criteria have been presented. For example, $H'_b=0.73$ (Boussinesq, 1842), $H'_b=0.78$ (McCown, 1891), $H'_b=0.83$ (Yamada, 1957) and $H'_b=0.75$ (Kishi, 1968). Recent researches reveal that the H'_b should be the function of slope, therefore the slope is derived into the criterion of related breaking wave height, e.g., Camfield & Street (1969), Grilli *et al.* (1944a, 1997) and Otta *et al.* (1993). However, these criteria seem to be satisfied only for slopes less than the slope $s=1:10$. $H'_b=0.78$ suggested by McCown is used in this paper as an index of a breaking wave. When related wave height, $H'=H/h$, is equal to 0.78, the water surface profiles are shown in Fig. 6. It indicates that waves break near shoreline. Referring to Fig. 1, these results agree well with the prediction by Street & Camfield. The breaking wave height H_b, depth and location of breaking wave, h_b and x_b, are listed in Table 3. Dean and Dalrymple (1984) derived the location of breaking wave x_b as

Table 2. Comparison for the Maximum Runup of Solitary Waves on the Slope s=1:1 and 1:2.

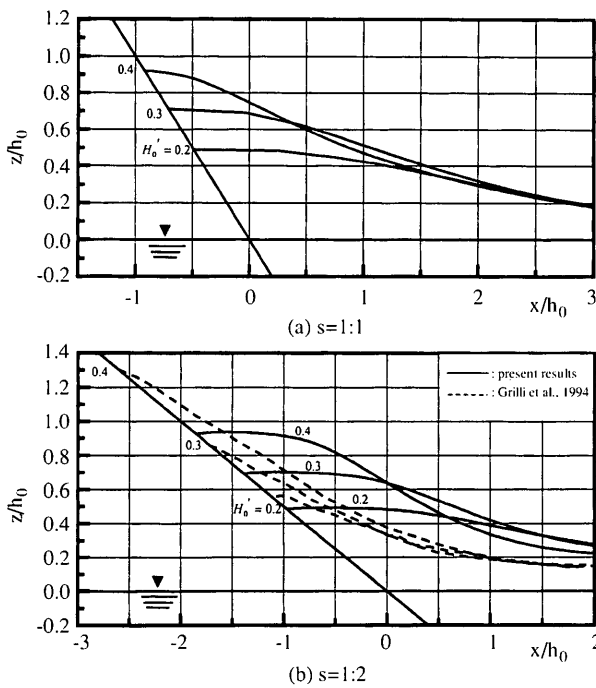|	s=1:1			s=1:2		
	H'=0.2	H'=0.3	H'=0.4	H'=0.2	H'=0.3	H'=0.4
Synolakis (1987)	0.38	0.63	0.90	0.54	0.89	1.27
Grilli (1994)				0.57	0.92	1.30
Present results	0.48	0.71	0.92	0.49	0.70	0.93

(a) s=1:1

(b) s=1:2

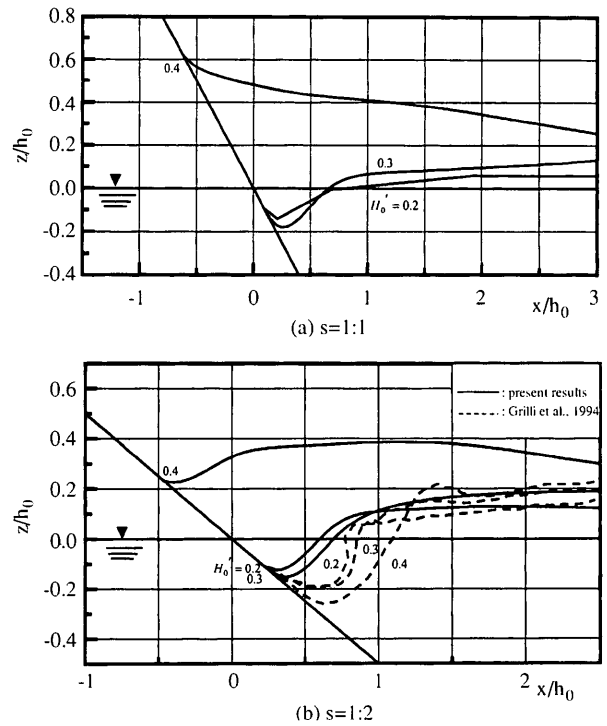Fig. 4. The water surface profiles for maximum runup.

(a) s=1:1

(b) s=1:2

Fig. 5. The water surface profiles for minimum rundown.

$$x_b = \frac{g^{1/5}}{\beta_*^{4/5}}(\frac{H_o'^2 T}{4\pi})^{2/5} \qquad (24)$$

where β_* is related breaking wave height and equal to 0.78. For the comparisons of the present results to the analytical results by Eq. (24) listed in Table 3, reasonable agreement is obtained.

4. The Distributions of Fluid Velocities for H_o' = 0.4 on Slopes

For the waves with H_o'=0.4 on slopes s=1:1, 1:2 and 1:5, the distributions of fluid velocities are investigated. To realize the characteristics of shoaling, we focus on the region near the slope.

The distributions of fluid velocities for the case of slope s=1:1 are shown in Fig. 7. When a wave reaches a coastal region, the fluid velocities in front of the crest increase due to the decrease of water depth. At maximum runup (t=6.48t_c), the fluid velocities become minimum because of the transformation from kinetic energy to potential energy. At this
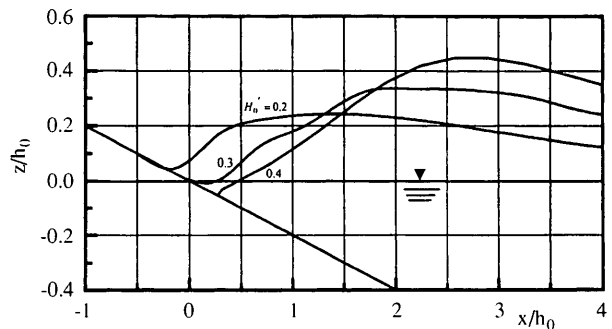

Fig. 6. The water surface profiles of solitary waves on slope s=1: 5 at H/h=0.78.

moment, the fluid velocities on the free water surface are almost along the water surface profile. During the process of backwash, the fluid velocities increase rapidly going offshore. At t=6.8t_c, the wave breaks due to the increase of fluid velocities near the shoreline that rush down to the seabed.

Table 3. The Location and Depth of Breaking Wave and Breaking Wave Height for Waves with $H_o' =$ 0.2~0.4 on Slope $s=1:5$

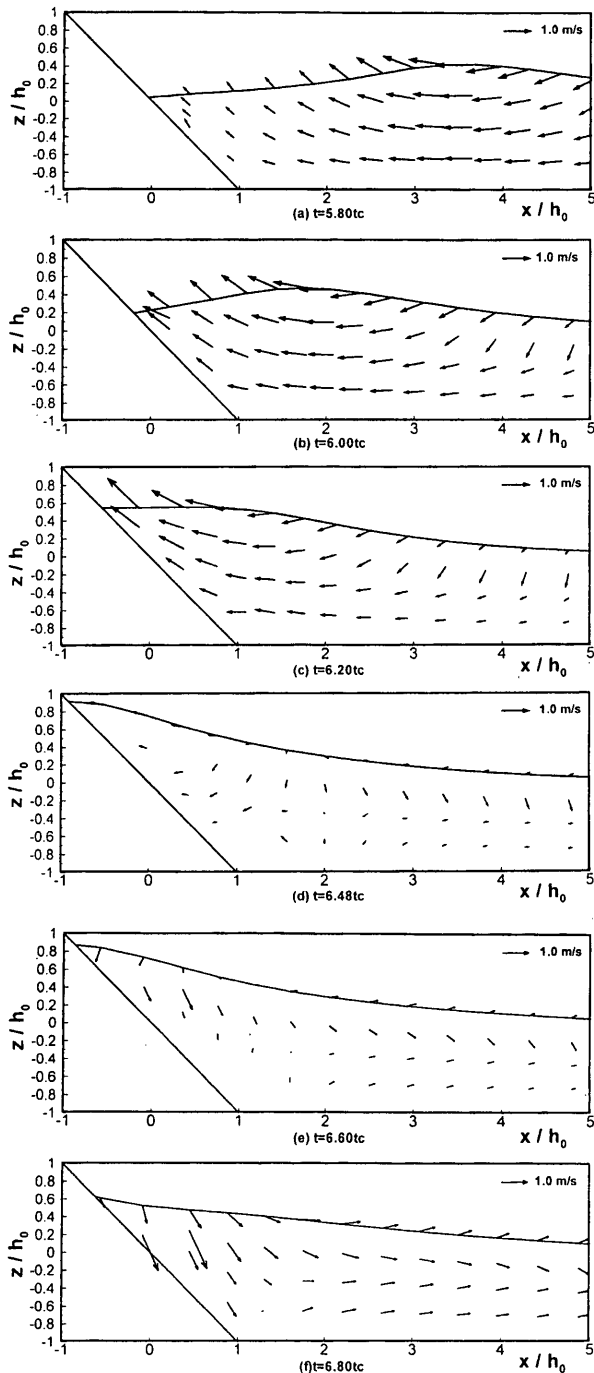|	$H_o'=0.2$		$H_o'=0.3$		$H_o'=0.4$	
	Dean & Dalrymple	present result	Dean & Dalrymple	present result	Dean & Dalrymple	present result
x_b	2.010	1.573	2.520	2.142	2.950	2.894
h_b	0.402	0.315	0.504	0.428	0.590	0.579
H_b	0.314	0.242	0.393	0.335	0.460	0.448

Fig. 7. The distributions of fluid velocities for wave with $H_o' =$ 0.4 on slope $s=1:1$.

Figure 8 represents the distributions of fluid velocities for the wave on slope $s=1:2$. Figure 9 shows distributions of fluid velocities for the wave on slope $s=1:5$. As the wave propagates on the slope, fluid velocities increase. At $t=6.5t_c$ H' is equal to 0.78, horizontal components of fluid velocities in front of the crest dominate and lead the wave break.

V. CONCLUSIONS

The processes of runup and rundown of solitary waves on slopes are simulated, the distributions of fluid velocities are also studied for waves with $H_o' =$ 0.4. Some conclusions are listed below:

1. For the waves that break during rundown, at breaking, the fluid velocities near the shoreline change the wave's direction and turn back toward shoreline. It is a possible reason why the wave breaks during rundown.
2. On slopes $s=1:1$ and $1:2$, waves with $H_o'=0.2$~0.4 propagate through the slope and break during rundown. For the case of $H_o'=0.2$ and 0.3, waves break under still water level. For $H_o'=0.4$, waves break above the still water level.
3. For waves on slope $s=1:1$, the values of dimensionless maximum runup R' agree well with the runup formula derived by Synolakis (1987).
4. The criterion of $H_b'=0.78$ is used to determine whether waves break. For the cases of $H_o'=0.2$~0.4 on slope $s=1:5$, waves break near shoreline. The location of breaking wave x_b is in reasonable agreement with the results of Dean & Dalrymple (1984).

NOMENCLATURE

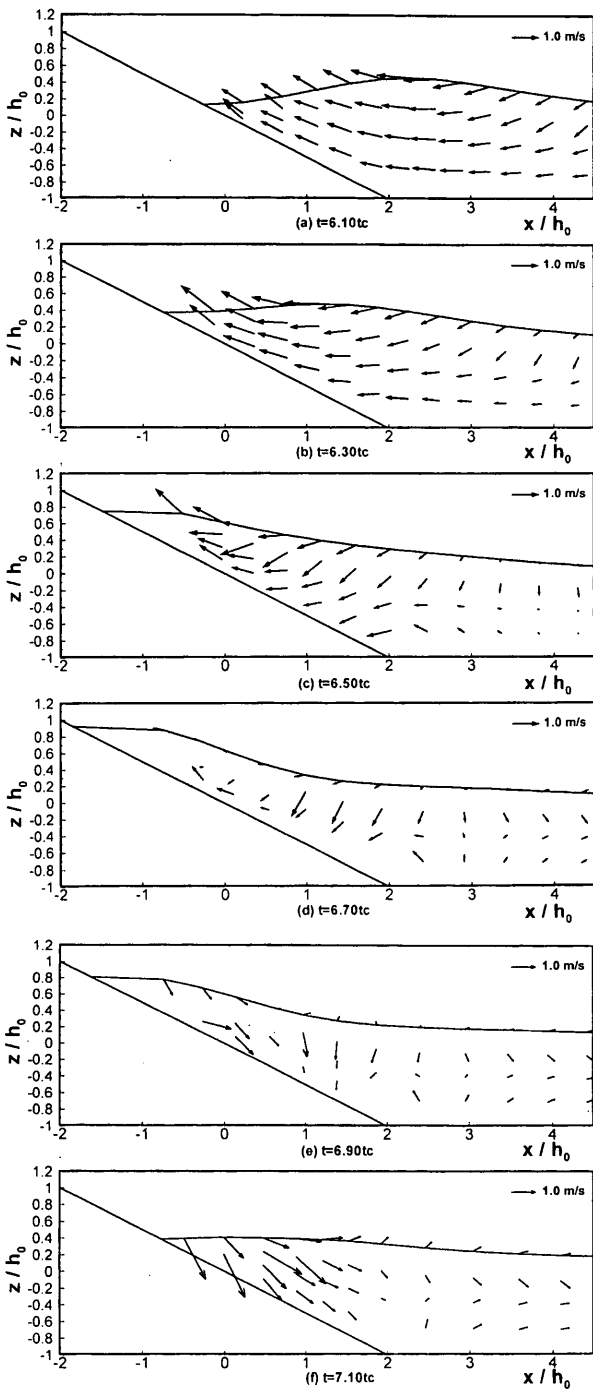|	
C_e	celerity of solitary wave
D	Lagrangian differentiation
g	gravitational acceleration
H	local solitary wave height
H_b	breaking wave height
H_b'	related breaking wave height
H_o	incident solitary wave height
H_o'	relative incident solitary wave height
h	local water depth

Fig. 8. The distributions of fluid velocities for wave with H'_o = 0.4 on slope s=1:2.
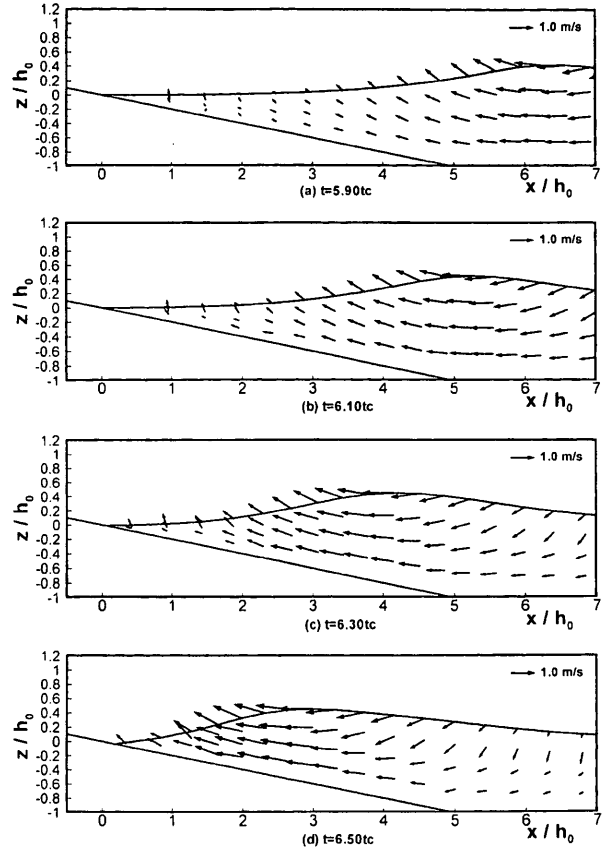
Fig. 9. The distributions of fluid velocities for wave with H'_o = 0.4 on slope s=1:5.

N_4	number of elements on bottom seabed
R	maximum runup
R'	dimensionless maximum runup
$\mathfrak{R}'$	dimensionless maximum runup derived by Synolakis
s	slope
T	period of solitary wave
t	time
t_c	characteristic time
Δt	time interval
U	horizontal moving velocity of wave generator
u	horizontal component of fluid velocity
w	vertical component of fluid velocity
x	horizontal coordinate
x_o	semistroke of paddle
z	vertical coordinate
β	angle of slope
Γ_1	boundary of pseudo wave generator
Γ_2	boundary of free water surface
Γ_3	boundary of slope
Γ_4	boundary of bottom seabed
Φ	velocity potential
ς	elevation of free water surface
ω	characteristic angular frequency

h_b	depth of breaking wave
h_o	water depth of constant water region
l	distance of constant water region
n	unit outward normal vector
N_1	number of elements on pseudo wave generator
N_2	number of elements on free water surface
N_3	number of elements on slope

REFERENCES

1. Camfield, F.E., and Street, R.L., 1969, "Shoaling of Solitary Waves on Small Slopes," *Journal of Waterway, Port, Coastal and Ocean Engineering*, ASCE, Vol. 95, No. 1, pp.1-22.
2. Chou, C.R., 1983, *The Boundary Element Method Applied to Waves*, Dept. of Harbor and River Eng. of Taiwan Ocean University, Keelung, R.O.C. (in Chinese).
3. Chou, C.R., and Shih, R.S., 1996, "Generation and Deformation of Solitary Waves," *China Ocean Engineering*, Vol. 10, No. 4, pp. 419-432.
4. Chou, C.R., Yueh, C.Y., and Weng, W.K., 1988, "Numerical Solution for Nonlinear Wave," *Proc. 10th Conference On Ocean Engineering. in R.O.C.*, pp. 617-627 (in Chinese).
5. Dean, R.G., and Dalrymple, R.A., 1984, *Water Wave Mechanics for Engineers and Scientists*, Prentice-Hall Inc., Englewood Cliffs, New Jersey.
6. Grilli, T.S., Losada, M.A., and Martin, F., 1994a, "Characteristics of Solitary Wave Breaking Induced by Breakwater," *Journal of Waterway, Port, Coastal and Ocean Engineering*, Vol. 120, pp. 74-92.
7. Grilli, S.T., Subramaya, R., Svendsen, I.A., and Eeramony, J., 1994b, "Shoaling of Solitary Waves on Plane Beaches," *Journal of Waterway, Port, Coastal and Ocean Engineering*, Vol. 120, No.6, pp. 609-628.
8. Grilli, S.T., Svendsen, I.A., and Subramaya, R., 1997, "Breaking Criterion and Characteristics for Solitary Waves on Slopes," *Journal of Waterway, Port, Coastal and Ocean Engineering*, Vol. 123, No. 3, pp. 120-112.
9. Kim, S.K., Liu, P.L.F., and Liggett, J.A., 1983, "Boundary Integral Equation Solutions for Solitary Wave Generation, Propagation and Runup," *Coastal Engineering*, 7, pp. 299-317.
10. Kobayashi, N., and Wurjanto, A., 1989, "Wave Overtopping on Coastal Structures," *Journal of Waterway, Port, Coastal and Ocean Engineering*, Vol. 115, No. 2, pp. 235-251.
11. Nakayama, T., 1983, "Boundary Element Analysis of Nonlinear Water Wave Problems," *International Journal for Numerical Methods in Engineering*, Vol. 19, pp. 953-970.
12. Otta, A.K., Svendsen, I.A., and Grilli, I.A., 1993, "The Breaking and Runup of Solitary Waves on Water," *Proc., 23rd International Conference on Coast. Engineering*, ASCE, Vol. 2, New York, N.K., pp.1461-1474.
13. Pedersen, G., and Gjevik, B., 1987, "Runup of Solitary Waves," *Journal of Fluid Mechanics*, Vol. 135, pp. 283-299.
14. Street, R.L., and Camfield, F.E., 1966, "Observations and Experiments on Solitary Wave Deformation," *Proc. 10th Conference Coastal Engineering*, pp. 284-301.
15. Synolakis, C.E., 1987, "The Runup of Solitary Waves," *Journal of Fluid Mechanics*, Vol. 185, pp. 523-545.

孤立波在陡坡溯升研究

周宗仁　歐陽寬

台灣海洋大學河海工程學系

摘　要

本文以邊界元素法建立一模擬非線性造波之數值水槽，探討孤立波於陡坡的溯升和溯降現象。配合自由水面的非線性邊界條件，本數值模式以Lagrangian法描述水粒子的運動，以前進差分法處理時間項的微分。孤立波達到最大溯升時的高度和自由水面波形將於本文中探討，並將結果與其他文獻的數據做比較。對相對入射波高等於0.4的孤立波，其流場的速度分佈亦被討論。

關鍵字：孤立波，溯上，碎波。